

Electronic correlations and unusual superconducting response in the optical properties of the iron-chalcogenide $\text{FeTe}_{0.55}\text{Se}_{0.45}$

C. C. Homes,* A. Akrap, J. S. Wen, Z. J. Xu, Z. W. Lin, Q. Li, and G. D. Gu
*Condensed Matter Physics and Materials Science Department,
Brookhaven National Laboratory, Upton, New York 11973, USA*
(Dated: April 13, 2021)

The in-plane complex optical properties of the iron-chalcogenide superconductor $\text{FeTe}_{0.55}\text{Se}_{0.45}$ have been determined above and below the critical temperature $T_c = 14$ K. At room temperature the conductivity is described by a weakly-interacting Fermi liquid; however, below 100 K the scattering rate develops a frequency dependence in the terahertz region, signalling the increasingly correlated nature of this material. We estimate the dc conductivity $\sigma_{dc}(T \gtrsim T_c) \simeq 3500 \pm 400 \Omega^{-1}\text{cm}^{-1}$ and the superfluid density $\rho_{s0} \simeq 9 \pm 1 \times 10^6 \text{cm}^{-2}$, which places this material close to the scaling line $\rho_{s0}/8 \simeq 8.1 \sigma_{dc} T_c$ for a BCS dirty-limit superconductor. Below T_c the optical conductivity reveals two gap features at $\Delta_{1,2} \simeq 2.5$ and 5.1 meV.

PACS numbers: 74.25.Gz, 74.70.Xa, 78.30.-j

The surprising discovery of superconductivity in the iron-arsenic $\text{LaFeAsO}_{1-x}\text{F}_x$ (“1111”) pnictide compound has prompted an intense investigation of this class of materials.^{1,2} The critical temperature T_c may be increased above 50 K through rare-earth substitutions.³ While the mechanism for superconductivity in many metals and alloys is mediated by lattice vibrations,⁴ the high values for T_c and the strong interplay between the magnetism and the lattice suggest that the superconductivity in this class of materials is not phonon mediated.⁵ In addition to searching for higher values of T_c in the 1111 family of materials, considerable effort has been made looking for superconductivity in other structurally-simpler Fe-based systems. In metallic BaFe_2As_2 the application of pressure yields $T_c \simeq 29$ K, while Co- and Ni-doping yields $T_c \simeq 23$ K at ambient pressure.⁶⁻⁸ Superconductivity has also been observed in the As-free iron-chalcogenide FeSe compound with $T_c = 8$ K, which increases to $T_c = 27$ K with the application of pressure.^{9,10} By introducing Te, the critical temperature in $\text{FeTe}_{1-x}\text{Se}_x$ at ambient pressure reaches a maximum $T_c = 14$ K for $x = 0.45$. Despite these structural differences, the band structure of these materials is similar, with a minimal description consisting of an electron band (β) at the M point and a hole band (α) at the center of the Brillouin zone.¹¹ There have been a number of studies of the Fe_{1+x}Te and $\text{FeTe}_{1-x}\text{Se}_x$ materials, including transport,¹²⁻¹⁵ tunneling¹⁶ and angle-resolved photoemission,¹⁷⁻²⁰ with particular emphasis placed on the magnetic properties.²⁰⁻²⁵ While the optical properties of the superconducting iron-pnictide materials have been investigated in some detail,²⁶⁻³² in comparison the iron-chalcogenide materials remain relatively unexplored.¹³

In this work we examine the in-plane complex optical properties of superconducting $\text{FeTe}_{0.55}\text{Se}_{0.45}$ above and below T_c . Over much of the normal state the material is a weakly-interacting Fermi liquid and the transport is Drude-like. However, close to T_c the Drude picture breaks down and the scattering rate adopts a strong fre-

quency dependence, signalling the increasingly correlated nature of this material.^{19,33} The onset of superconductivity is clearly observed in the optical properties below T_c , and the optical conductivity suggests that in addition to a prominent gap feature at $\simeq 5.1$ meV, a second gap opens at $\simeq 2.5$ meV.

Single crystals with good cleavage planes (001) were grown by a unidirectional solidification method with a nominal composition of $\text{FeTe}_{0.55}\text{Se}_{0.45}$ and a critical temperature determined by magnetic susceptibility of $T_c = 14$ K with a transition width of $\simeq 1$ K. The reflectance from the cleaved surface of a mm-sized single crystal has been measured at a near-normal angle of incidence for several temperatures above and below T_c over a wide frequency range (~ 2 meV to 4 eV) for light polarized in the a - b planes using an *in situ* overcoating technique.³⁴ The reflectance in the terahertz and far-infrared region (1 THz = 33.4cm^{-1}) is shown in Fig. 1 (the extended unit cell of FeTe is shown in the inset). At room temperature, the reflectance displays the typical metallic form in the Hagen-Rubens regime $R \propto 1 - \sqrt{\omega}$; however, just above T_c the reflectance develops a striking linear frequency dependence. Below T_c the formation of a superconducting condensate and the opening of a gap in the spectrum of excitations is clearly visible. The reflectance is a complex quantity consisting of an amplitude and a phase, $\tilde{r} = \sqrt{R}e^{i\theta}$; because only the amplitude $R = \tilde{r}\tilde{r}^*$ is measured it is often not intuitively obvious what changes in the reflectance imply. Consequently, the complex optical properties have been determined from a Kramers-Kronig analysis of the reflectance.³⁵

The temperature dependence of the real part of the optical conductivity is shown in Fig. 2 in the infrared region; the far-infrared region is shown in the inset. At room temperature, the conductivity is relatively flat and structureless, except for a sharp feature associated with the infrared-active E_u mode at 204cm^{-1} which is due to the in-plane displacements of the Fe-Te(Se) atoms³⁶ (slightly higher than the E_u mode observed at 187cm^{-1} in our examination of $\text{Fe}_{1.03}\text{Te}$). As the temperature is

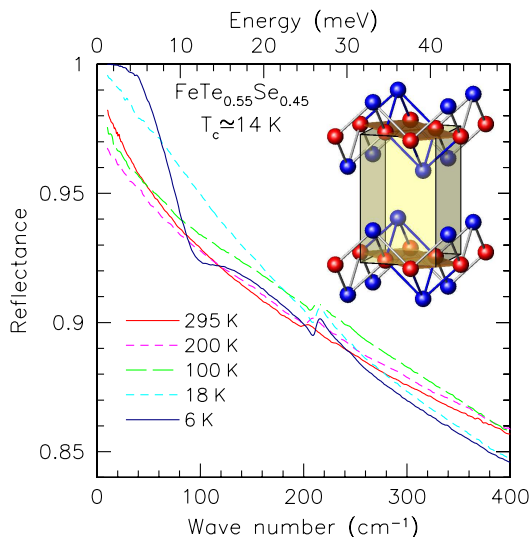


FIG. 1. (Color online) The reflectance of $\text{FeTe}_{0.55}\text{Se}_{0.45}$ in the far infrared region for light polarized in the Fe-Te planes at several temperatures above and below T_c . Inset: The extended unit cell of FeTe in the tetragonal $P4/nmm$ space group showing the tetrahedrally-coordinated Te above and below the Fe planes.

lowered there is a redistribution of the spectral weight [defined here as the weight under the conductivity curve over a given interval, $\int_{0^+}^{\omega_c} \sigma_1(\omega, T) d\omega$] from high to low frequency. This response is not unusual for a metallic system where the scattering rate decreases with temperature. The optical conductivity is described by a Drude-Lorentz model for the dielectric function $\tilde{\epsilon} = \epsilon_1 + i\epsilon_2$,

$$\tilde{\epsilon}(\omega) = \epsilon_\infty - \frac{\omega_{p,D}^2}{\omega^2 + i\omega/\tau_D} + \sum_j \frac{\Omega_j^2}{\omega_j^2 - \omega^2 - i\omega\gamma_j}, \quad (1)$$

where ϵ_∞ is the real part of the dielectric function at high frequency, $\omega_{p,D}^2 = 4\pi n e^2 / m^*$ and $1/\tau_D$ are the plasma frequency and scattering rate for the delocalized (Drude) carriers, respectively; ω_j , γ_j and Ω_j are the position, width, and strength of the j th vibration or excitation. The complex conductivity is $\tilde{\sigma}(\omega) = \sigma_1 + i\sigma_2 = -i\omega[\tilde{\epsilon}(\omega) - \epsilon_\infty]/4\pi$.

The optical conductivity may be reproduced quite well using this approach at 295, 200 and 100 K, with fitted values of $\omega_{p,D} = 7200 \text{ cm}^{-1}$ and $1/\tau_D = 414, 363$ and 317 cm^{-1} , respectively ($\pm 5\%$). To fit the midinfrared component, Lorentzian oscillators at the somewhat arbitrary positions of 650 and 3000 cm^{-1} have been introduced, allowing the free-carrier component to be fit using a single Drude expression, as opposed to the two-Drude response that has recently been applied to some of the pnictide materials.³² While this approach works well over most of the normal state, it fails for the optical conductivity just above T_c at 18 K, where the low-frequency component is not Drude-like. To address this problem, we consider the extended-Drude model in which the scattering rate takes on a frequency dependence. The

experimentally-determined scattering rate is³⁷

$$\frac{1}{\tau(\omega)} = \frac{\omega_p^2}{4\pi} \text{Re} \left[\frac{1}{\tilde{\sigma}(\omega)} \right]. \quad (2)$$

In this instance we set $\omega_p = \omega_{p,D}$ and $\epsilon_\infty = 4$ [although the choice of ϵ_∞ has little effect upon $1/\tau(\omega)$ in the far-infrared region]; the temperature dependence of $1/\tau(\omega)$ is shown in Fig. 3 above and below T_c . At 295, 200 and 100 K the scattering rate displays little frequency dependence, and moreover $1/\tau(\omega \rightarrow 0) \simeq 1/\tau_D$. This self-consistent behavior indicates that within this temperature range, the transport may be described as a weakly-interacting Fermi liquid (Drude model). However, just above T_c at 18 K the scattering rate develops a linear frequency dependence $\lesssim 200 \text{ cm}^{-1}$, suggesting strong electronic correlations.¹⁹ This may be due in part to magnetic correlations²¹ that arise from the suppression of the magnetic transition in $\text{Fe}_{1+\delta}\text{Te}$ at $T_N \simeq 70 \text{ K}$ in response to Se substitution.¹⁴ We note that similar behavior of the scattering rate is observed in optimally-doped cuprates where the electronic correlations may have a similar origin.³⁸ Dramatic changes are also observed in $1/\tau(\omega)$ below T_c where the scattering rate is suppressed at low frequencies, but increases rapidly and overshoots the normal-state (18 K) value at about 60 cm^{-1} , finally merging with the normal-state curve at about 200 cm^{-1} ; this behavior is in rough agreement with a recently proposed sum rule for the scattering-rate.³⁹

Returning to the optical conductivity in Fig. 2, below T_c there is a dramatic suppression of the low-frequency conductivity and a commensurate loss of spectral weight which is shown in more detail in the inset. The loss

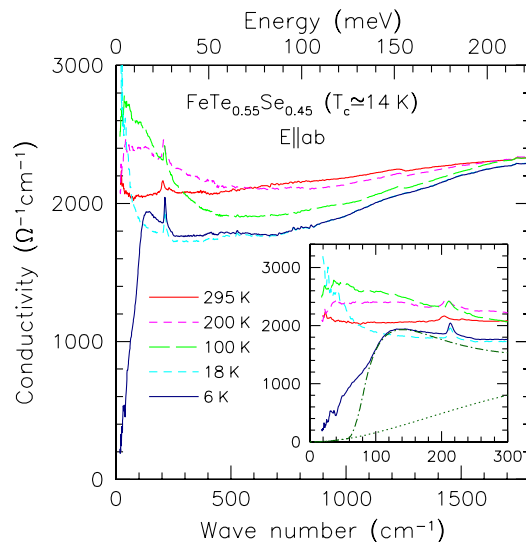


FIG. 2. (Color online) The real part of the in-plane optical conductivity for $\text{FeTe}_{0.55}\text{Se}_{0.45}$ at several temperatures above and below T_c in the infrared region. Inset: The conductivity in the far-infrared region compared with a model calculation for a single isotropic gap ($\Delta_0 = 4.5 \text{ meV}$, $1/\tau = 4\Delta_0$) superimposed on the Lorentzian contribution.

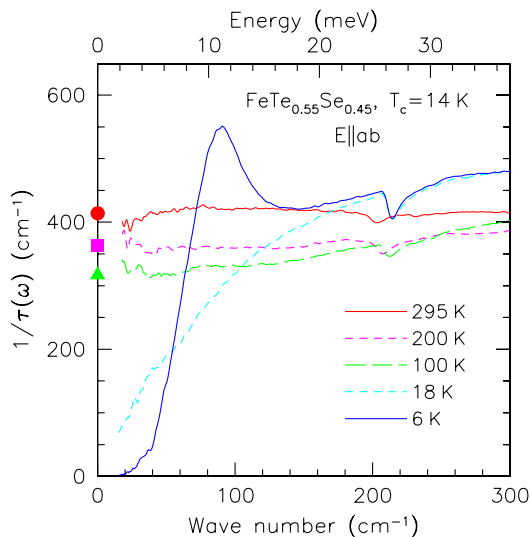


FIG. 3. (Color online) The in-plane frequency-dependent scattering rate of $\text{FeTe}_{0.55}\text{Se}_{0.45}$ for several temperatures above and below T_c in the far-infrared region. The values for $1/\tau_D$ are shown at 295 (●), 200 (■) and 100 K (▲), respectively, where the scattering rate displays little temperature dependence. For $T \gtrsim T_c$ (18 K) at low frequency $1/\tau(\omega) \propto \omega$, while for $T < T_c$ large changes in the scattering rate are observed in response to the formation of superconducting gap(s).

of spectral weight is associated with the formation of a superconducting condensate, whose strength may be calculated from the Ferrell-Glover-Tinkham sum rule: $\int_{0+}^{\omega_c} [\sigma_1(\omega, T \gtrsim T_c) - \sigma_1(\omega, T \ll T_c)] d\omega = \omega_{p,S}^2/8$. Here $\omega_{p,S}^2 = 4\pi n_s e^2/m^*$ is the superconducting plasma frequency and the cut-off frequency $\omega_c \simeq 150 \text{ cm}^{-1}$ is chosen so that the integral converges smoothly; the superfluid density is $\rho_{s0} \equiv \omega_{p,S}^2$. The sum rule yields $\omega_{p,S} = 3000 \pm 200 \text{ cm}^{-1}$, indicating that less than one-fifth of the free-carriers in the normal state have condensed ($\omega_{p,S}^2/\omega_{p,D}^2 \lesssim 0.18$). The superfluid density can also be expressed as an effective penetration depth $\lambda_0 = 5300 \pm 300 \text{ \AA}$, which is in good agreement with recent tunnel-diode measurement on $\text{FeTe}_{0.63}\text{Se}_{0.37}$ (Ref. 40). From the estimate $\sigma_{dc} \equiv \sigma_1(\omega \rightarrow 0) = 3500 \pm 400 \text{ \Omega}^{-1}\text{cm}^{-1}$ for $T \gtrsim T_c$, this compound is observed to fall on the general scaling line⁴¹ for a BCS superconductor with the condition that $1/\tau \gtrsim 2\Delta$ (the “dirty limit”), $\rho_{s0}/8 \simeq 8.1 \sigma_{dc} T_c$.

The detailed optical conductivity below T_c at 6 K is shown in Fig. 4. In addition to the strong suppression of the conductivity below $\sim 120 \text{ cm}^{-1}$, there is also a prominent shoulder at $\sim 60 \text{ cm}^{-1}$. Below T_c the optical conductivity has been calculated using a Mattis-Bardeen formalism for the contribution from the gapped excitations,^{35,42} as well as the low-frequency tail of the bound midinfrared excitations modeled by Lorentzian oscillators. The Mattis-Bardeen approach assumes that $l \lesssim \xi_0$, where the mean-free path $l = v_F \tau$ (v_F is the Fermi velocity), and the coherence length is $\xi_0 = \hbar v_F / \pi \Delta_0$ for an isotropic superconducting gap Δ_0 ; this may also be

expressed as $1/\tau \gtrsim 2\Delta_0$. This approach is motivated by the observation that less than one-fifth of the free carriers collapse into the condensate, a condition which indicates that these materials are not in the clean limit. Initially, only a single isotropic gap $\Delta_0 \simeq 4.5 \text{ meV}$ was considered; however, this failed to accurately reproduce the residual conductivity observed at low-frequency (inset in Fig. 2). To properly model the optical conductivity, two gaps at $\Delta_1 \simeq 2.5 \text{ meV}$ and $\Delta_2 \simeq 5.1 \text{ meV}$ are used. For the purposes of this calculation we have assumed a moderate amount of disorder scattering, $1/\tau_j = 4\Delta_j$. The optical conductivity for each of the gaps is shown in Fig. 4 for $T = 0$; the smoothed linear combination of the gaps and the Lorentzian tails is in good agreement with the experimental data. The observation of two gap features is consistent with a number of recent theoretical works that propose that s -wave gaps form on each band, possibly with a sign change between them (s^\pm), in this model the gap on the electron band may be an extended s -wave with nodes.^{43,44} The strong reduction of the conductivity at low frequency for $T \ll T_c$ suggests the absence of nodes. It is possible that disorder may lift the nodes, resulting in a nodeless extended s -wave gap.^{45,46} The optical results provide estimates of the gap amplitudes, but do not distinguish between s^\pm and extended s -wave. The optical gaps $2\Delta_j \simeq 40$ and 82 cm^{-1} are similar to or larger than the low-frequency scattering rate observed at 18 K, $1/\tau(\omega \rightarrow 0) \simeq 40 \text{ cm}^{-1}$. While this might seem to cast doubt on the validity of the Mattis-Bardeen approach, we note that the strong frequency dependence of the scattering rate at this temperature complicates mat-

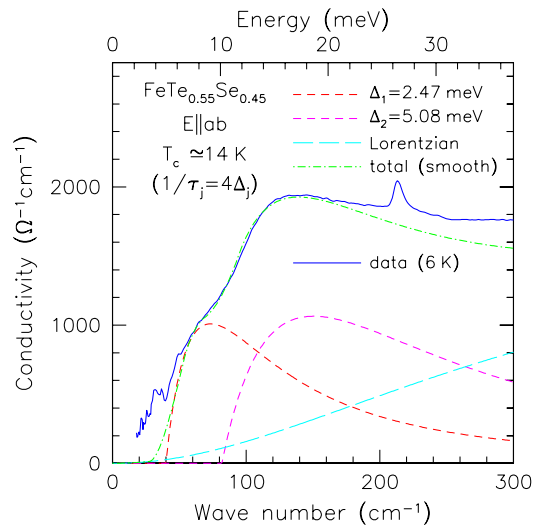


FIG. 4. (Color online) The in-plane optical conductivity of $\text{FeTe}_{0.55}\text{Se}_{0.45}$ shown at 6 K (solid line). The calculated optical conductivity with gaps of $2\Delta_1 \simeq 5 \text{ meV}$ and $2\Delta_2 \simeq 10.2 \text{ meV}$ for $T \ll T_c$ (short-dashed lines) is superimposed on the contribution from the bound excitations in the mid-infrared (long-dashed line); the smoothed linear combination of the three curves (dot-dash line) is in good agreement with the measured data below 200 cm^{-1} .

ters. If we consider the value of the $1/\tau(\omega)$ in the region of the optical gaps $2\Delta_j$ where the scattering should be important, we find from Fig. 3 that the scattering rate is then larger than the gap amplitude,

$$\frac{1/\tau_j(2\Delta_j)}{2\Delta_j} \approx 3,$$

which is actually larger than the ratio used in the calculation, indicating that the Mattis-Bardeen approach is correct. Finally, we note that while $2\Delta_1/k_B T_c \simeq 4$ is close to the value of 3.5 expected in the BCS weak-coupling limit,⁴ $2\Delta_2/k_B T_c \simeq 8.4$ is significantly larger.

To summarize, the optical properties of FeTe_{0.55}Se_{0.45} ($T_c = 14$ K) have been examined for light polarized in the Fe-Te(Se) planes above and below T_c . Well above T_c the transport may be described by a weakly-interacting Fermi liquid (Drude model); however, this picture breaks

down close to T_c when the scattering rate takes on a strong frequency dependence, similar to what is observed in the cuprate superconductors. Below T_c , less than one-fifth of the free carriers collapse into the condensate ($\lambda_0 \simeq 5300$ Å), indicating that this material is in the dirty limit, and indeed this material falls on the general scaling line predicted for a BCS dirty-limit superconductor. To successfully model the optical conductivity, two gaps of $\Delta_1 \simeq 2.5$ meV and $\Delta_2 \simeq 5.1$ meV are considered using a Mattis-Bardeen formalism (with moderate disorder scattering), suggesting either an s^\pm or an nodeless extended s -wave gap.

We would like to acknowledge useful discussions with D. N. Basov, J. P. Carbotte, A. V. Chubukov and J. M. Tranquada. This work is supported by the Office of Science, U.S. Department of Energy (DOE) under Contract No. DE-AC02-98CH10886.

* homes@bnl.gov

- ¹ Y. Kamihara, T. Watanabe, M. Hirano, and H. Hosono, *J. Am. Chem. Soc.* **130**, 3296 (2008).
- ² K. Ishida, Y. Nakai, and H. Hosono, *J. Phys. Soc. Japan* **78**, 062001 (2009).
- ³ Z.-A. Ren, J. Yang, W. Lu, W. Yi, X.-L. Shen, Z.-C. Li, G.-C. Che, X.-L. Dong, L.-L. Sun, F. Zhou, and Z.-X. Zhao, *EPL* **82**, 57002 (2008).
- ⁴ J. Bardeen, L. N. Cooper, and J. R. Schrieffer, *Phys. Rev.* **108**, 1175 (1957).
- ⁵ L. Boeri, O. V. Dolgov, and A. A. Golubov, *Phys. Rev. Lett.* **101**, 026403 (2008).
- ⁶ P. L. Alireza, Y. T. C. Ko, J. Gillett, C. M. Petrone, J. M. Cole, G. G. Lonzarich, and S. E. Sebastian, *J. Phys.: Condens. Matter* **21**, 012208 (2009).
- ⁷ A. S. Sefat, R. Jin, M. A. McGuire, B. C. Sales, D. J. Singh, and D. Mandrus, *Phys. Rev. Lett.* **101**, 117004 (2008).
- ⁸ L. J. Li, Q. B. Wang, Y. K. Luo, H. Chen, Q. Tao, Y. K. Li, X. Lin, M. He, Z. W. Zhu, G. H. Cao, and Z. A. Xu, *New J. Phys.* **11**, 025008 (2009).
- ⁹ F.-C. Hsu, J.-Y. Luo, K.-W. Yeh, T.-K. Chen, T.-W. Huang, P. M. Wu, Y.-C. Lee, Y.-L. Huang, Y.-Y. Chu, D.-C. Yan, and M.-K. Wu, *Proc. Nat. Acad. Sci. U.S.A.* **105**, 14262 (2008).
- ¹⁰ Y. Mizuguchi, F. Tomioka, S. Tsuda, T. Yamaguchi, and Y. Takano, *Appl. Phys. Lett.* **93**, 152505 (2008).
- ¹¹ S. Raghu, X.-L. Qi, C.-X. Liu, D. J. Scalapino, and S.-C. Zhang, *Phys. Rev. B* **77**, 220503(R) (2008).
- ¹² M. H. Fang, H. M. Pham, B. Qian, T. J. Liu, E. K. Vehstedt, Y. Liu, L. Spinu, and Z. Q. Mao, *Phys. Rev. B* **78**, 224503 (2008).
- ¹³ G. F. Chen, Z. G. Chen, J. Dong, W. Z. Hu, G. Li, X. D. Zhang, P. Zheng, J. L. Luo, and N. L. Wang, *Phys. Rev. B* **79**, 140509(R) (2009).
- ¹⁴ B. C. Sales, A. S. Sefat, M. A. McGuire, R. Y. Jin, D. Mandrus, and Y. Mozharivskyj, *Phys. Rev. B* **79**, 094521 (2009).
- ¹⁵ T. Taen, Y. Tsuchiya, Y. Nakajima, and T. Tamegai, *Phys. Rev. B* **80**, 092502 (2009).
- ¹⁶ T. Kato, Y. Mizuguchi, H. Nakamura, T. Machida,

- H. Sakata, and Y. Takano, *Phys. Rev. B* **80**, 180507(R) (2009).
- ¹⁷ Y. Xia, D. Qian, L. Wray, D. Hsieh, G. F. Chen, J. L. Luo, N. L. Wang, and M. Z. Hasan, *Phys. Rev. Lett.* **103**, 037002 (2009).
- ¹⁸ K. Nakayama, T. Sato, P. Richard, T. Kawahara, Y. Sekiba, T. Qian, G. F. Chen, J. L. Luo, N. L. Wang, H. Ding, and T. Takahashi, arXiv:0907.0763 (unpublished).
- ¹⁹ A. Tamai, A. Y. Ganin, E. Rozbicki, J. Bacsá, W. Meevasana, P. D. C. King, M. Caffio, R. Schaub, S. Margadonna, K. Prassides, M. J. Rosseinsky, and F. Baumberger, *Phys. Rev. Lett.* **104**, 097002 (2010).
- ²⁰ S.-H. Lee, Guangyong Xu, W. Ku, J. S. Wen, C. C. Lee, N. Katayama, Z. J. Xu, S. Ji, Z. W. Lin, G. D. Gu, H.-B. Yang, P. D. Johnson, Z.-H. Pan, T. Valla, M. Fujita, T. J. Sato, S. Chang, K. Yamada, and J. M. Tranquada, arXiv:0912.3205 (unpublished).
- ²¹ J. Wen, G. Xu, Z. Xu, Z. W. Lin, Q. Li, W. Ratcliff, G. Gu, and J. M. Tranquada, *Phys. Rev. B* **80**, 104506 (2009).
- ²² Y. Qiu, W. Bao, Y. Zhao, C. Broholm, V. Stanev, Z. Tesanovic, Y. C. Gasparovic, S. Chang, J. Hu, B. Qian, M. Fang, and Z. Mao, *Phys. Rev. Lett.* **103**, 067008 (2009).
- ²³ R. Khasanov, M. Bendele, A. Amato, P. Babkevich, A. T. Boothroyd, A. Cervellino, K. Conder, S. N. Gvasaliya, H. Keller, H.-H. Klauss, H. Luetkens, V. Pomjakushin, E. Pomjakushina, and B. Roessli, *Phys. Rev. B* **80**, 140511(R) (2009).
- ²⁴ M. J. Han and S. Y. Savrasov, *Phys. Rev. Lett.* **103**, 067001 (2009).
- ²⁵ W. Bao, Y. Qiu, Q. Huang, M. A. Green, P. Zajdel, M. R. Fitzsimmons, M. Zhernenkov, S. Chang, M. Fang, B. Qian, E. K. Vehstedt, J. Yang, H. M. Pham, L. Spinu, and Z. Q. Mao, *Phys. Rev. Lett.* **102**, 247001 (2009).
- ²⁶ W. Hu, Q. Zhang, and N. Wang, *Physica C* **469**, 545 (2009).
- ²⁷ J. Yang, D. Hüvonen, U. Nagel, T. Rööm, N. Ni, P. C. Canfield, S. L. Bud'ko, J. P. Carbotte, and T. Timusk, *Phys. Rev. Lett.* **102**, 187003 (2009).
- ²⁸ K. W. Kim, M. Rössle, A. Dubroka, V. K. Malik, T. Wolf,

- and C. Bernhard, arXiv:0912.0140 (unpublished).
- ²⁹ M. Nakajima, S. Ishida, K. Kihou, Y. Tomioka, T. Ito, Y. Yoshida, C. H. Lee, H. Kito, A. Iyo, H. Eisaki, K. M. Kojima, and S. Uchida, *Phys. Rev. B* **81**, 104528 (2010).
- ³⁰ E. van Heumen, Y. Huang, S. de Jong, A.B. Kuzmenko, M.S. Golden, and D. van der Marel, arXiv:0912.0636 (unpublished).
- ³¹ B. Gorshunov, D. Wu, A. A. Voronkov, P. Kallina, K. Iida, S. Haindl, F. Kurth, L. Schultz, B. Holzapfel, and M. Dressel, *Phys. Rev. B* **81**, 060509(R) (2010).
- ³² D. Wu, N. Barišić, P. Kallina, A. Faridian, B. Gorshunov, N. Drichko, L. J. Li, X. Lin, G. H. Cao, Z. A. Xu, N. L. Wang, and M. Dressel, *Phys. Rev. B* **81**, 100512(R) (2010).
- ³³ M. Qazilbash, J. J. Hamlin, R. E. Baumbach, L. Zhang, D. J. Singh, M. B. Maple, and D. N. Basov, *Nature Phys.* **5**, 647 (2009).
- ³⁴ C. C. Homes, M. Reedyk, D. A. Cradles, and T. Timusk, *Appl. Opt.* **32**, 2976 (1993).
- ³⁵ M. Dressel and G. Grüner, *Electrodynamics of Solids* (Cambridge University Press, Cambridge, 2001).
- ³⁶ T.-L. Xia, D. Hou, S. C. Zhao, A. M. Zhang, G. F. Chen, J. L. Luo, N. L. Wang, J. H. Wei, Z.-Y. Lu, and Q. M. Zhang, *Phys. Rev. B* **79**, 140510(R) (2009).
- ³⁷ A. Puchkov, D. N. Basov, and T. Timusk, *J. Phys.: Condens. Matter* **8**, 10049 (1996).
- ³⁸ D. N. Basov and T. Timusk, *Rev. Mod. Phys.* **77**, 721 (2005).
- ³⁹ D. N. Basov, E. J. Singley, and S. V. Dordevic, *Phys. Rev. B* **65**, 054516 (2002).
- ⁴⁰ H. Kim, C. Martin, R. T. Gordon, M. A. Tanatar, J. Hu, B. Qian, Z. Q. Mao, Rongwei Hu, C. Petrovic, N. Salovich, R. Giannetta, and R. Prozorov, arXiv:1001.2042 (unpublished).
- ⁴¹ C. C. Homes, S. V. Dordevic, M. Strongin, D. A. Bonn, R. Liang, W. N. Hardy, S. Komiya, Y. Ando, G. Yu, N. Kaneko, X. Zhao, M. Greven, D. N. Basov, and T. Timusk, *Nature (London)* **430**, 539 (2004); C. C. Homes, S. V. Dordevic, T. Valla, and M. Strongin, *Phys. Rev. B* **72**, 134517 (2005).
- ⁴² W. Zimmermann, E. Brandt, M. Bauer, E. Seider, and L. Genzel, *Physica C* **183**, 99 (1991).
- ⁴³ I. I. Mazin, D. J. Singh, M. D. Johannes, and M. H. Du, *Phys. Rev. Lett.* **101**, 057003 (2008).
- ⁴⁴ A. V. Chubukov, D. V. Efremov, and I. Eremin, *Phys. Rev. B* **78**, 134512 (2008).
- ⁴⁵ V. Mishra, G. Boyd, S. Graser, T. Maier, P. J. Hirschfeld, and D. J. Scalapino, *Phys. Rev. B* **79**, 094512 (2009).
- ⁴⁶ J. P. Carbotte and E. Schachinger, *Phys. Rev. B* **81**, 104510 (2010).